

Analysis of Liquid Flow-Induced Motion of a Discrete Solid in a Partially Filled Pipe

Bal M. Mahajan

National Bureau of Standards, Washington, DC 20234

Accepted: April 20, 1983

An analysis is presented for the liquid flow-induced motion of a solid in partially filled pipes. A general equation of the flow-induced motion of a solid is developed. Two alternate force models, one (F_v) based on free stream velocity and another (F_m) based on free stream momentum flux, are formulated to simplify the general equation.

The equation of motion is solved for the motion of a cylindrical solid with steady-uniform liquid flows and the effects of relevant variables on the motion of a solid are predicted. The variables considered include: volume rate of liquid flow, Q ; pipe diameter, D ; Manning coefficient, n ; and slope, S ; solid diameter, d ; length, L ; specific gravity, σ ; coefficient of friction between a solid and the pipe wall, η ; and the two force functions, F_v and F_m .

The flow rate, Q , required to initiate the motion of a solid increases with an increase in D , n , d , L , σ , and η , and decreases with an increase in S . The force function F_m predicts a lower value of Q than does the force function F_v .

The velocities of a solid increase with an increase in Q and S and decrease with an increase in D , n , d , L , σ , and η . The force function F_m predicts higher values of the velocity of a solid than does the force function F_v .

The effects of the variables Q , D , S , d , L , and η on the velocities of a solid are qualitatively consistent with the available experimental data. The qualitative agreement between the predicted results and experimental data demonstrate the validity of the analysis presented.

Key words: analysis; flow; force; liquid; model; momentum; partially-filled; pipe; solid; solid-liquid channel flow; steady; uniform; velocity.

1. Introduction

The transport of solids by flowing liquids falls into three different categories: (1) the sediment transport in rivers and canals—the sediment particles usually move on the river bed and do not block the passage of the flow or alter the cross-sectional area of the flow; (2) the pipeline transport of finite solids and particle suspensions by full-bore liquid flows—the flow parameters (velocity, volume flow rate, and pressure) of the carrier liquid are relatively easy to obtain since the pipe is completely filled with the liquid; (3) the pipeline transport of solids by flowing liquids only partially filling the pipe (open channel flows)—the flow parameters (velocity, volume rate of flow, and flow depth) of carrier liquid are relatively difficult to obtain. (The difficulty is encountered even for a constant volume flow rate because the flow velocity and depth may vary along the length of the pipe; furthermore, the transported solid may substantially alter the flow area and the solid may or may not be fully submerged.)

About the Author: Bal M. Mahajan is a mechanical engineer in the NBS Center for Building Technology.

Nomenclature

<p>A = flow cross-sectional area</p> <p>A_s = cross-sectional area of solid</p> <p>A_{sw} = wetted portion of the cross-sectional area of the solid</p> <p>A_w = portion of the pipe's cross-sectional area occupied by the water, or the flow cross-sectional area</p> <p>C_l = lift coefficient</p> <p>C_r = coefficient of flow-induced force</p> <p>d = diameter of the solid</p> <p>D = diameter of the pipe</p> <p>E = flow specific energy</p> <p>F_b = buoyant force</p> <p>F_f = friction force</p> <p>F_l = lift force</p> <p>F_m = force function based on free stream momentum flux</p> <p>F_p = pressure force</p> <p>Fr = Froude number</p> <p>F_s = shear force</p> <p>F_v = force function based on free stream velocity</p> <p>F_{ws} = flow-induced thrust force acting on the solid</p> <p>g = acceleration due to gravity</p> <p>h = depth of water stream</p> <p>L = length of the solid</p> <p>m = mass of the solid</p> <p>n = the Manning coefficient</p> <p>P_w = wetted perimeter</p> <p>P_{sw} = wetted perimeter of the solid</p> <p>p = pressure</p> <p>Q = volume flow rate</p> <p>R = A/P_w = hydraulic radius</p> <p>R_n = normal reaction, force due to pipe wall acting on the solid in a direction perpendicular to the pipe axis</p> <p>S = pipe slope = $\sin\theta$</p> <p>S_f = energy gradient or slope of the energy line</p> <p>T = time</p> <p>U = solid velocity</p>	<p>V = water velocity</p> <p>V_{wd} = volume of water displaced by the solid</p> <p>W_b = buoyed weight of the solid</p> <p>W_s = weight of the solid</p> <p>X_s = axial distance traversed by a solid</p> <p>x = x-axis or the axial distance along the length of the pipe</p> <p>y = y-axis or the distance perpendicular to the pipe axis</p> <p style="text-align: center;"><i>Greek Symbols</i></p> <p>α = acceleration</p> <p>γ = specific weight</p> <p>η = friction coefficient</p> <p>ϵ = y/d and/or h/d</p> <p>θ = pipe slope angle</p> <p>λ = y/D and/or h/D</p> <p>ν = $V_o - U_m$</p> <p>ρ = density</p> <p>σ = specific gravity</p> <p>τ_{sw} = average value of shear stress due to water flow on the solid</p> <p style="text-align: center;"><i>Subscripts</i></p> <p>m refers to maximum value</p> <p>o refers to free stream condition</p> <p>p, p refers to pipe or pressure</p> <p>s refers to solid</p> <p>t refers to instantaneous values</p> <p>v refers to free stream quantity</p> <p>1 refers to nose or upstream end of the solid</p> <p>2 refers to tail or downstream end of the solid</p>
---	--

The first two categories of solid transport by flowing liquids have been investigated extensively [1,2]¹, while the third category has received relatively little attention. Situations involving the transport of solids with partially filled pipe flows are common occurrences in gravity drainage systems and in some aspects of the chemical industry.

Recently, transport of discrete solids in partially filled pipes was experimentally investigated at the National Bureau of Standards (NBS) [3,4]. In these experiments, single cylindrical solids were transported by unsteady (surge type) water flows in slightly pitched horizontal pipes and the effects of selected variables on the velocity (U_s) of the solid were examined. The variables considered in the experiments were: the volume of water (V_w) used in an experiment, diameter (D) and slope (S) of the pipe, diameter (d) and length (L) of the solid, and the coefficient of static friction (η_s) between the solid and the pipe wall. The data of these experiments indicated that: (1) at any given cross-section of the pipe, U_s increases with an increase in V_w and S , and a decrease in D , d , L , η_s ; (2) U_s first increases, apparently reaches a maximum value, and then starts to decrease as the solid travels downstream; and (3) the difference between the local maximum velocity (V_m) of water and the U_s appears to be a function of the axial distance from the solid's starting location and all of the selected variables.

Recent experimental studies at NBS and in several foreign countries [3-8] have enhanced the understanding of the water flow-induced motion of discrete solids in partially filled pipes. These studies have also revealed the complexities of the mechanism of momentum exchange between the liquid and solid and the dissipation of flow energy. Formulation and selection of rational momentum exchange or force models are essential steps for developing techniques for predicting the motion or transport of discrete solids in partially filled pipes under all flow conditions.

This paper presents an analysis of the liquid flow-induced motion of a discrete solid in a partially filled pipe. Various forces acting on the solid are discussed and a general equation for the axial motion of the solid is developed.

This general equation is also shown to be applicable to the liquid flow-induced motion of a discrete solid in a pipe flowing full. Two simplified force models are formulated. The simplified equation is used to study the motion of a finite cylindrical solid for steady-uniform flows. The effects of utilizing different force models and of relevant variables on the various states of the motion of the solid are examined. The variables considered for this parametric study include the following: volume rate of steady uniform flow; coefficient of friction between the solid and the pipe wall; variables of the pipe (i.e., pipe diameter, slope, and the Manning coefficient); and the variables of the solid (i.e., diameter, length, and specific gravity).

The three states of the motion of the solid investigated are: (1) the threshold conditions, i.e., the effects of the variables on the threshold flow rate or the minimum value of flow rate required to initiate the motion of a solid are examined; (2) the acceleration of a solid from rest to the equilibrium velocity, i.e., the effects of the variables on the velocity of a solid along the length of the pipe are examined; and (3) the equilibrium conditions, i.e., the effect of the variables on the equilibrium velocity of the solid are examined.

2. Analysis

2.1 Types of Partially Filled Pipe Flows

Before considering the transport of a solid by liquid in partially filled pipes (or open channel flows in pipes), it is instructive to briefly describe the types of open channel flows that may occur in nominally horizontal or slightly pitched horizontal pipes. Partially filled pipe flows are classified as: steady or unsteady according to the changes in flow parameters with respect to time, T , and uniform or varied according to the changes in flow parameters with respect to distance, x , along the length of the pipe [9,10]. In general, there are three basic types of partially filled pipe flows: (1) steady-uniform flows; (2) steady-varied flows; and (3) unsteady or unsteady-varied flows.

¹ Figures in brackets indicate literature references at the end of this paper.

Establishment of unsteady-uniform flows is practically impossible [9,10]. Also, considering the effects of gravity the state of a partially filled pipe flow may be subcritical (Froude number, Fr , less than unity), critical (Fr equal to unity), or supercritical (Fr greater than unity). These three basic types of flow can be further described as follows:

Steady-uniform flows. The flow parameters, that is volume flow rate or discharge Q , depth h , and velocity V , do not vary with respect to both T and x . Also, the energy line, water surface, and pipe axis are parallel. Any one of the flow parameters (Q , h , or V) completely define the flow conditions for a given pipe, i.e., if Q is given, h and V can be easily determined by the use of the Chezy or Manning formula [9,10].

Steady-varied flows. The flow may be either gradually or rapidly varied. For steady varied flows, Q is constant with respect to both T and x , but h and V are constant only with respect to T and vary with X . The energy line, water surface, and pipe axis are not parallel. There are several (about 12 for gradually varied flows) possible water surface profiles or flow profiles for steady varied flows. For given value of Q through a pipe, values of h and V at any section of the pipe may be determined by numerical integration of the steady-varied flow equations.

Unsteady flows. Unsteady flows may be either gradually varied unsteady flows or rapidly varied unsteady flows. Short duration unsteady flows through slightly-pitched-pipes, as in horizontal branches of gravity drainage systems when a plumbing fixture is discharged into the drains serving the fixture, are often called surge flows. For surge flows, the volume flow rate of the liquid entering the pipe rises rapidly from zero to a peak value, and then gradually falls off to zero. A surge flow attenuates as it moves downstream, i.e., the peak values of the flow parameters decrease with an increase in axial distance from the pipe inlet.

For unsteady flow, the flow parameters vary with both T and x . Also, the energy line, water surface, and pipe axis are not parallel. Owing to their complexity, the exact solutions of the unsteady flow equations are not possible. However, various finite difference schemes have been developed to obtain approximate solutions of the unsteady flow equations. Numerical integration techniques applying the method of characteristics may be used to estimate the attenuation of a surge flow along the length of the pipe and to obtain approximate values of the flow parameters [5,9–13].

The application of such finite difference techniques has been the subject of a parallel study at NBS to investigate the motion of solids in partially filled pipes [8]. In this approach, motion of the solid is predicted by an empirical equation linking the disturbed flow depth across the solid to its velocity and other flow parameters. The flow-induced motion of a solid predicted by this technique is qualitatively consistent with the observed data.

2.2 Description of Liquid-Solid Interaction and the Motion of a Solid

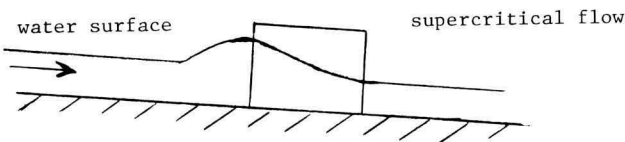
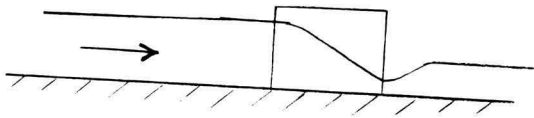
Let us visualize what happens in the case of a single cylindrical solid, initially at rest in a slightly pitched horizontal pipe, as a partially filled pipe flow approaches the solid. The stationary solid partially blocks the flow and the liquid rushes through the crescent shaped space between the solid and the pipe wall. In addition, when an open channel flow is obstructed by the presence of an obstacle (such as a bridge pier, dam, sluice gate, or a weir), the depth of the liquid surface upstream of the obstacle becomes greater than it would have been for unobstructed flow. This phenomenon is called the “backwater” effect of the obstruction on the flow and has been studied by many researchers, see, for example, references [9] and [10].

The extent of this effect is greatly dependent upon the size of the obstruction and the state of the flow. Flow at the obstruction is either subcritical or supercritical [9,10]. For example, if the obstructed flow is subcritical, the backwater will extend a long distance upstream relative to the dimensions of the obstruction (fig. 1). If the flow is supercritical and the obstruction is relatively small, the water surface adjacent to the upstream end of the obstruction is disturbed and the disturbance does not extend further upstream. However, a relatively large obstruction may cause the upstream water level to rise above the critical depth and cause the backwater effect to extend

a short distance upstream (fig. 1); this backwater profile may be terminated by a hydraulic jump. The backwater effect of solids on the flow was observed during the recent experimental study by the author [3,4]; this effect is shown in figure 2.

As a result of the backwater effect, there is a buildup of some water upstream of the solid causing a hydrostatic head difference along the solid. Also, curvature of the stream lines around the upstream end (or the nose) of the solid may increase the flow velocity at that point. Eddies may be formed along the sides and in front (downstream) of the solid as indicated in figure 3.

The stationary solid, in addition to its weight, is also subjected to the following water flow-induced forces in the downstream direction: (1) a pressure force due to the unequal water depth and unequal velocity along the opposite ends of the solid; and (2) a shear force due to the streaming of water past the solid. The solid is also subjected to similar forces due to the induced air flow in the pipe; the effect of air flow related forces, however, is negligibly small. In addition, the solid is also subjected to a buoyancy force, a reaction force at the solid-pipe contact surface, and a force due to the friction between the solid and the pipe wall.

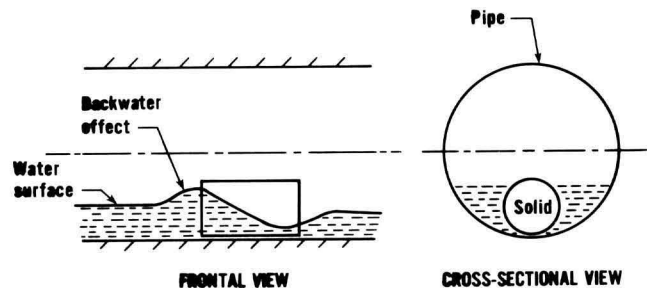
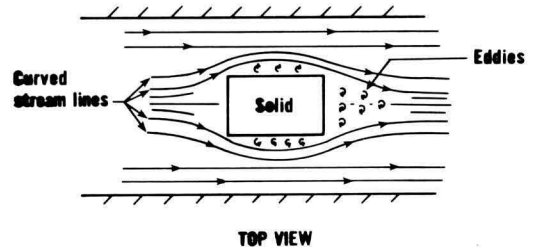
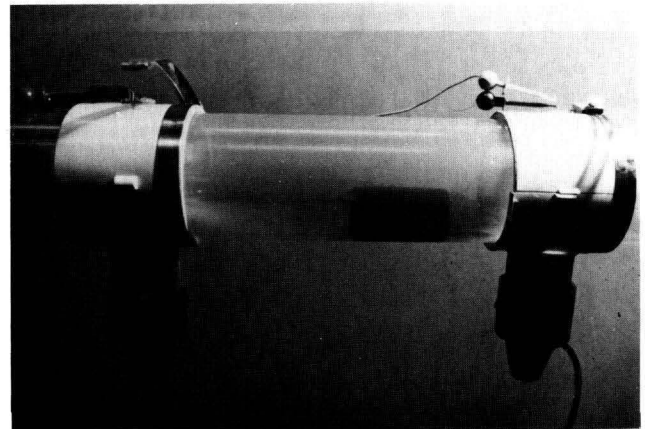


(Clockwise from above)

Figure 1—Schematic of the backwater effect of an obstruction on an open channel flow.

Figure 2—Photograph showing the “backwater effects” of a solid on the partially-filled pipe flow.

Figure 3—Schematic of a cylindrical solid in a partially-filled pipe flow showing eddies and backwater effects.



The result of these forces may not act at the solid's center of gravity, thus producing a net moment which may cause a slight upward tilt of the nose of the solid, a slight lateral displacement of the solid, or both. Any shift in the position of the solid would cause changes in the magnitude and in the line of action of the forces acting on the solid. As a result, the solid may oscillate with respect to its original position for a while or it may take up a new position so that the net moment is zero. However, for the force analysis of the flow-induced motion of the solid it will be assumed that the axis of the solid remains parallel to the pipe axis.

The magnitude of the liquid flow-induced forces acting on the solid increases with an increase in the liquid flow rate through the pipe. The solid remains stationary until the sum of forces acting in the downstream direction exceeds the force due to static friction between the solid and the pipe wall. Once this friction force is exceeded, the solid starts to move. The instantaneous water flow rate, which is just sufficient to start the motion of the solid, is called the "threshold flow rate," and corresponding flow parameters are called "threshold flow parameters."

When the solid is in motion, the friction force is reduced because the coefficient of sliding friction is less than that of static friction. The pressure and shear forces acting on the solid in the downstream direction are also reduced because of a decrease in relative velocity between the water and the solid. The shear force over some parts of the solid surface may even reverse in direction if the solid velocity is higher than the local liquid velocity. This situation is likely to occur near the interface between the bottom of the pipe and the solid. The eddies along the side of the solid and the flow in the thin water layer between the solid and pipe invert may also give rise to a lift force, causing a further reduction in the friction force. As a consequence, the solid accelerates and/or decelerates until it attains an "equilibrium velocity" and a balance of forces develops. The "equilibrium velocity" of the solid (except for steady-uniform liquid flows), does not have a constant value because the velocity of the carrier fluid for steady-varied and surge flows is not constant along the length of the pipe. During the motion of the solid, if the solid velocity is not equal to the local liquid velocity, the liquid continues to flow past the solid.

The solid will continue to move with the equilibrium velocity as long as there is sufficient liquid influx to balance the forces acting on the solid. However, if the flow of carrier fluid through the pipe is of steady-varied or surge flow type, then the liquid flow-induced forces acting on the solid may decrease as the solid moves downstream due to a decrease in the liquid velocity, liquid depth, or both. As a consequence of the decrease in the forces, the solid decelerates, from equilibrium velocity and may come to rest.

In general, there are three different phases of liquid flow-induced motion of a solid in partially filled pipes: (1) the solid accelerates from rest to equilibrium velocity; (2) the solid continues to move at the equilibrium velocity; and (3) the solid decelerates from the equilibrium velocity, particularly if the carrier fluid flow is of steady-varied or surge flow type.

2.3 Force Balance and Equations of Motion

The analysis presented below is one-dimensional and deals with the water flow-induced motion of the solid in the downstream direction. Also, it is assumed that the axis of the solid remains parallel to the pipe axis, i.e., any shift of the position of the solid with respect to the pipe axis is neglected.

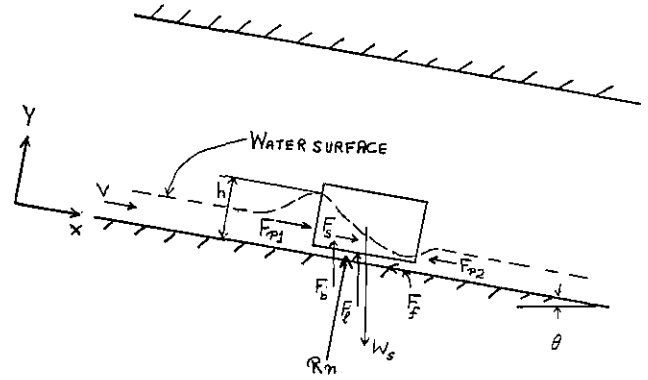
Various forces acting on a cylindrical solid due to water flow in a partially filled pipe were described in the previous subsection. These forces and the coordinate axes are shown in figure 4. Summation of x - and y -component of forces yield the following:

$$\Sigma F_x = F_{p1} - F_{p2} + F_s + W_s \sin\theta - F_f - F_b \sin\theta - F_l \sin\theta = ma \quad (1)$$

$$\Sigma F_y = R_n - W_s \cos\theta + F_b \cos\theta + F_l \cos\theta = 0 \quad (2)$$

where the symbols are defined in the nomenclature. The brief descriptions and mathematical formulations of the force terms are given below.

Figure 4—Forces acting on a solid in a pipe flowing only partially full.



The buoyant force, F_b , is taken equal in magnitude to the weight of water displaced by the solid. (Due to local flow acceleration, F_b may actually be somewhat less than the weight of the displaced liquid.) It acts in a vertical direction and its line of action passes through the centroid of the volume of water, V_{wd} , displaced by the solid. Both the magnitude of F_b and the location of its line of action will vary with the variations in the magnitude and shape of V_{wd} . Since the stream depth varies along the length of the solid, the magnitude of F_b may be expressed as:

$$F_b = \rho g \int_{x_1}^{x_2} A_{sw} dx = \rho g V_{wd} = \rho g L \bar{A}_{sw} \quad (3)$$

where \bar{A}_{sw} = the value of the wetted cross-sectional area of the solid averaged over L (the length of the solid).

The friction force, F_f , is due to the friction between the solid and the pipe wall in the presence of water. The value of F_f is at maximum when the motion of the solid is impending. The magnitude of F_f decreases when the solid starts to move because the coefficient of dynamic friction is less than that of static friction. The magnitude of F_f will decrease further if a lift force is generated and it will be equal to zero when R_n is zero. The value of F_f may be found as:

$$F_f = \eta R_n, \text{ or substituting } R_n \text{ from eq (2)}$$

$$F_f = \eta \{ (W_s - F_b) - F_\ell \} \cos \theta = \eta (W_b - F_\ell) \cos \theta \quad (4)$$

where

$$W_b = (W_s - F_b) = \rho g L [\sigma A_s - \bar{A}_{sw}] \quad (5)$$

The lift force, F_ℓ , depends on the water solid interaction. It is due to the flow-produced forces on the solid in a direction upward from the pipe wall. Its magnitude and center of action will depend upon the density and size of the solid, the size of the pipe, and the local characteristics of the flow. Force F_ℓ may be assumed to act in a direction parallel to F_b and it further reduces the magnitude of W_b . The magnitude of F_ℓ may be assumed to vary between zero to a maximum value of W_b . The force F_ℓ may be written as:

$$F_\ell = C_\ell W_b \quad (6)$$

where C_ℓ is a lift coefficient which is a function of the flow velocity relative to the solid. The value of C_ℓ varies between zero and one; however at the present state of knowledge, C_ℓ cannot be predicted from theory alone.

The pressure forces F_{p1} and F_{p2} , respectively, act on the nose (upstream end) and tail (downstream end) of the solid. The magnitude of pressure forces is dependent on the water depth which is dependent upon the size of the pipe, depth of the flow stream, and the relative velocity between the solid and water. The pressure forces F_{p1} and F_{p2} may be written as follows:

$$F_{p1} = \rho g [\bar{y} + U_r^2/2g]_1 A_{sw1} \quad (7)$$

$$F_{p2} = \rho g [\bar{y} + U_r^2/2g]_2 A_{sw2} \quad (8)$$

where subscripts 1 and 2, respectively, refer to the nose and tail of the solid.

$U_r = V - U =$ relative velocity between the solid and the water

\bar{y} = the distance from the water surface to the centroid of the wetted cross-sectional area of the solid, A_{sw} .

For a right circular cylindrical solid situated with its axis parallel to the axis of the pipe as shown in figure 3, \bar{y} may be expressed as:

$$\bar{y} = \left(\int_0^h y dA_{sw} \right) / A_{sw} = d \{ [2d^2(\epsilon - \epsilon^2)^{3/2} / 3A_{sw}] - (1 - 2\epsilon) / 2 \} \quad (9)$$

where

$$A_{sw} = \int_0^h dA_{sw} = [\cos^{-1}(1 - 2\epsilon) - 2(1 - 2\epsilon)\sqrt{\epsilon - \epsilon^2}] d^2 / 4 \quad (10)$$

$\epsilon = y/d$, and y equal to the distance of the water surface from the bottom of the solid. If the solid is in contact with the pipe, then \bar{y} may also be expressed as:

$$\bar{y} = \left[\int_0^h y dA_w \right] / A_w = D \{ [2D^2(\lambda - \lambda^2)^{3/2} / 3A_w] - (1 - 2\lambda) / 2 \} \quad (11)$$

and

$$A_w = \int_0^h dA_w = [\cos^{-1}(1 - 2\lambda) - 2(1 - 2\lambda)\sqrt{1 - \lambda^2}] D^2 / 4 \quad (12)$$

where $\lambda = h/D$, and h is the distance of the water surface from the bottom of the pipe.

The net pressure force, F_p , acting on the solid in the downstream direction (or x -direction) may be obtained as:

$$F_p = F_{p1} - F_{p2} = \rho g \{ [\bar{y} + U_r^2/2g]_1 A_{sw1} - [\bar{y} + U_r^2/2g]_2 A_{sw2} \} \quad (13)$$

The shear force F_s acts over the entire wetted surface of the solid in a direction parallel to the direction of flow. The shear force is dependent upon the size of the solid, the surface roughness of the solid, the depth of flow stream, relative velocity between the solid and the water, and water viscosity. The shear force F_s may be expressed in a formulation similar to the formulation of the shear force acting on the flow due to pipe friction (or boundary layer shear). The velocity and depth of flow varies along the length of the solid, and F_s may be formulated in terms of the average values of the variables averaged over the length of the solid as:

$$F_s = \tau_{sw} L \bar{P}_{sw} \quad (14)$$

where

$$\bar{P}_{sw} = \frac{1}{L} \int_{x_1}^{x_2} P_{sw} dx = \cos^{-1}(1 - 2\epsilon)d = \text{average value of wetted perimeter of the solid, averaged over}$$

L , and

τ_{sw} = average value of shear stress due to water flow on the solid.

The relationship of the shear stress, τ_{sw} , to the local flow parameters is not known and needs development.

Substituting the expressions for various force terms from eqs (3), (4), (5), (13), and (14), the equations of motion for the solid may be rewritten as:

$$\rho\{[g\bar{y} + U_r^2/2]_1 A_{sw1} - [g\bar{y} + U_r^2/2]_2 A_{sw2}\} + \tau_{sw} L \bar{P}_{sw} + W_b \sin\theta(1-C_r) - \eta W_b \cos\theta(1-C_r) = m\alpha \quad (15)$$

Equation (15) is free from any assumption regarding the shape or size of the solid or the type of liquid flow in the pipe. Various terms have been formulated for a right circular cylindrical solid in motion or at rest in a pipe partially filled with flowing water; however, eq (15) gives the force balance on a discrete solid of any shape or size moving or at rest in a pipe totally filled or partially filled with flowing liquid.

For example let us examine the case of a right circular cylinder at rest in a pipe filled with flowing liquid; for this case.

$$\alpha = 0, C_r = 0,$$

$$A_{sw1} = A_{sw2} = \pi d^2/4,$$

$$\bar{y}_1 = \bar{y}_2 = d/2,$$

$$\bar{P}_{sw} = \pi d,$$

$$U_{r1} = V_1, U_{r2} = V_2 \text{ and}$$

$$(V_1^2 - V_2^2)/2 = \Delta P \text{ across the solid.}$$

Now substituting these values in eq (15) we get

$$\rho \Delta P A_s = \tau_{sw} L P + W_b \sin\theta - \eta W_b \cos\theta \quad (16)$$

Equation (16), when adjusted for proper direction of various forces, is identical to eq (12-54) of reference [2]. For a cylindrical solid moving with a steady speed in a pipe filled with flowing liquid, eq (15) becomes identical to eq (12-71) of reference [2], after proper directions of the forces are taken into consideration.

2.4 Force Models to Simplify the Equation of Motion

Equation (15) may be further simplified by combining the flow-induced pressure and shear forces to obtain a longitudinal flow-induced thrust force acting on the solid as:

$$F_{ws} - W_b(1-C_r)[\eta \cos\theta - \sin\theta] = m\alpha \quad (17)$$

where,

$$F_{ws} = F_p + F_s = \rho C_f [U_{r1}^2] A_{sw1} / 2 \quad (18)$$

and where C_f is a coefficient of the flow-induced force acting on the solid and is expressed by the following:

$$C_f = (2/U_{r1}^2 A_{sw1}) [g\bar{y} + U_r^2/2]_1 A_{sw1} - (g\bar{y} + U_r^2/2)_2 A_{sw2} + \tau_{sw} L \bar{P}_{sw} \quad (19)$$

To further simplify eq (19), the force F_{ws} and the buoyed weight, W_b , of the solid may be expressed:

$$F_{ws} = \rho C_f [U_{ro}^2/2] A_{swo} \quad (20)$$

$$W_b = \rho g L [\sigma A_s - A_{swo}] \quad (21)$$

where

$$U_{ro} = V_o - U$$

A_{swo} = area of the nose of the solid wetted by the free stream depth, h_o defined as the stream depth corresponding to the free stream velocity V_o .

The quantity V_o is the "free stream velocity," that is, the average velocity of water in the absence of a solid. For a steady uniform flow, V_o is the free stream velocity of flow in the pipe; for a steady (constant flow rate) gradually varied flow, V_o is the free stream velocity at location x_1 ; i.e., the axial distance corresponding to the position of the nose of the solid in the pipe; and for an unsteady, or surge flow, V_o is the free stream velocity at location x_1 and at time T_1 , i.e., the time at which the nose of the solid is at location x_1 .

The quantity C_f is a coefficient of thrust based on the "free stream velocity." The coefficient C_f is similar to a well known quantity C_d , "the coefficient of drag," for submerged bodies in infinite flow streams; here the subscript r is used to emphasize the thrust force exerted by the flowing liquid on the solid and the finite size of the flow field. Also, the effects of a solid on an infinite flow field are negligible and the drag coefficient, C_d , is taken as independent of the quantity A_{swo}/A_{wo} (i.e., the ratio of the wetted cross-section area of the solid and the free stream flow area). Depending on the cross-section areas, the effect of a solid on a partially filled pipe flow may be substantial and should be taken into consideration. Hence, the thrust force coefficient C_f is considered to be dependent upon the quantity A_{swo}/A_{wo} .

The exact relationship between C_f and A_{swo}/A_{wo} is complex even for a steady uniform flow condition. The approximate value of F_{ws} may be obtained by assuming that the coefficient C_f can be expressed as:

$$C_f = 1 + A_{swo}/A_{wo} \quad (22)$$

Substituting C_f from eq (22) into eq (20), F_{ws} or F_v may be expressed as:

$$F_{ws} = F_v = \rho [1 + A_{swo}/A_{wo}] [U_{ro}^2/2] A_{swo} \quad (23)$$

where F_v is the flow-induced force acting on the solid, the subscript v is used to indicate that the force is based upon free stream velocity.

The validity of the assumed expression for C_d may be examined by considering the following two limiting conditions: (a) the solid in an infinite flow field; and (b) the solid completely blocking the flow.

For the first case, when $A_{w_0} \rightarrow \infty$; then $A_{s_{w_0}}/A_{w_0} \rightarrow 0$. In this case,

$$F_v \rightarrow \rho[U_{ro}^2/2] A_{s_{w_0}} \quad (24)$$

Equation (24) represents the approximate value of the drag force acting on the cylinder in an infinite flow field with its axis parallel to the free stream velocity, since C_d for such a cylinder is nearly equal to unity [13].

For the second case, when $A_{s_{w_0}} \rightarrow A_{w_0}$; then $A_{s_{w_0}}/A_{w_0} \rightarrow 1$. In this case,

$$F_v = \rho[U_{ro}^2] A_{s_{w_0}} \quad (25)$$

Equation (25) represents the case of a jet impinging on a flat plate, where the force acting on the solid (i.e., the flat plate) is equal to the total flow momentum relative to the solid [14,15].

Substituting for W_b and F_v from eqs (21) and (23), respectively, the equation of motion for the solid, i.e., eq (17) may be rewritten as:

$$\rho(1 + A_{s_{w_0}}/A_{w_0})(U_{ro}^2/2) A_{s_{w_0}} - \rho g L (\sigma A_s - A_{s_{w_0}}) [\eta \cos \theta - \sin \theta] (1 - C_d) = m a \quad (26)$$

An alternate expression for the longitudinal flow-induced force, F_{ws} , acting on the solid may be obtained by considering the "momentum flux" or "specific force," M , of the free stream impinging on the solid as discussed below.² The momentum flux, M , of an open channel flow is defined as:

$$M = [\int y dA + QV/g] = (\bar{v} + V^2/g) A_w \quad (27)$$

Force F_{ws} may be expressed as

$$F_{ws} = F_m = \rho g (\bar{v} + U_{ro}^2/g) A_{s_{w_0}} - F_2 \quad (28)$$

where F_m is the flow-induced force acting on the solid, the subscript m is used to indicate that the force function is based upon the free stream momentum flux, and F_2 represents the force acting on the downstream end of the solid.

When $U_s = 0$, $U_{co} = V$ and

$$F_{ws} = F_m = \rho g (\bar{v} + V^2/g) A_{s_{w_0}} - F_2 \quad (29)$$

The first term on the right-hand side of eq (29) represents the force of an open channel flow on an obstruction, such as a sluice gate or a bridge pier, if the force F_2 is negligible. Such a situation is likely to occur only initially when the flowing liquid first contacts the solid. However, as soon as some liquid flowing through the crescent shaped space between the solid and the pipe wall reaches the downstream end of the solid, the liquid fills the portion of the pipe cross-section adjacent to the bottom of the pipe to form a region of eddies as shown in figure 3. The velocity

² The quantity M has been variously called the "momentum flux," the "specific force," the "momentum function," the "total force," the "force plus momentum," or briefly the "force" of a stream [9,10].

relative to the solid of the liquid adjacent to the downstream end of the solid is zero; the depth of this liquid is smaller than the free stream depth except when the buoyed weight of the solid is zero. When the buoyed weight of the solid is equal to zero then the depth of liquid adjacent to the downstream end of the solid is equal to the free stream depth. Hence, it may be assumed that the force F_2 is a hydrostatic force having a value equal to a fraction of the free stream hydrostatic force as:

$$F_2 = \rho g \left(\frac{A_{swo}}{\sigma A_s} \right) \bar{y} A_{swo}. \quad (30)$$

Substituting F_2 from eq.(30) into eq (28), eq (28) may be rewritten as:

$$F_m = F_{ws} = \rho g \left(1 - \frac{A_{swo}}{\sigma A_s} \right) \bar{y}_o A_{swo} + \rho U_{ro}^2 A_{swo}. \quad (31)$$

The first term on the right-hand side of eq (31) is equal to the net hydrostatic force acting on the solid and is equal to zero when W_b is equal to zero.

Substituting for W_b and F_{ws} , respectively, from eqs (21) and (31), eq (17) may be rewritten as:

$$\rho g \left(1 - \frac{A_{swo}}{\sigma A_s} \right) A_{swo} + \rho U_{ro}^2 A_{swo} - \rho g L (\sigma A_s - A_{swo}) [\eta \cos \theta - \sin \theta] (1 - C_r) = m \alpha. \quad (32)$$

A comparison of eqs (23) and (31) indicates that at identical flow conditions, the magnitude of force F_m is larger than that of force F_v .

Considering the force and mass balance for the water over the length of the pipe, L , containing the solid, the continuity and momentum equations for water may be expressed as follows:

$$\text{continuity, } Q_1 - Q_2 = \partial / \partial T \int_{x_1}^{x_2} A dx = (\partial A / \partial T) L; \quad (33)$$

$$\text{momentum, } \rho g (M_1 - M_2) + \rho g \bar{A}_w \sin \theta L - \rho g \bar{A}_w L S_f - F_{sw} = -\rho \frac{\partial}{\partial T} (A_w V) L \quad (34)$$

where

$$M = (\bar{y} + V^2/g) A_w,$$

$$S_f = \tau_{pw} / \gamma R = V^2 / C^2 R = n^2 V^2 / R^{4/3},$$

$$\rho g A L \sin \theta = W_w \sin \theta$$

τ_{pw} = average shear stress due to pipe on the water flow,

and

$F_{sw} = -F_{ws}$ = the flow resistive force exerted by the solid, and F_{ws} has already been defined in eqs (18), (23), or (31).

Now, if the solid is of infinitesimal length, then eqs (33) and (34) take up the more familiar forms, i.e., the equation for unsteady flow in open channels, e.g.,

when,

$L = \Delta x \rightarrow dx$, then

$$\partial Q / \partial x + \partial A / \partial T = 0 \quad (35)$$

or

$$\rho \partial M / \partial x + \rho g \bar{A}_w (S_o - S_f) - \partial (F_{sw}) / \partial x = -\rho \partial Q / \partial T. \quad (36)$$

Also, the resistance due to the solid may be expressed in a manner similar to the flow resistance due to the pipe wall as:

$$\partial (F_{sw}) / \partial x = \rho g A_w S_{fs}$$

and eq (23) may be rewritten as:

$$\rho \partial M / \partial x - \rho g \bar{A}_w (S_o - S_f - S_{fs}) = -\rho \partial Q / \partial T \quad (37)$$

where S_{fs} may be expressed in a manner similar to S_f , as

$$S_{fs} \approx \bar{U}_r^2 / C_s^2 R \approx n_s^2 U_r^2 / R^{4/3},$$

however, in this case coefficients C_s and n_s are not constant and are not known. In the absence of a solid, eq (37) becomes

$$\rho g \partial M / \partial x + \rho \partial Q / \partial T = \rho g A_w (S - S_f) \quad (38)$$

For steady uniform partially filled pipe flows, parameters, Q , V , and h , are constant throughout the pipe; and for a given value of Q , the values of u and h can be determined using the Manning equation [9,10]. Also, for given values of Q , pipe variables (D, n, S), and solid variables (d, L, σ), the force F_{ws} varies only with the solid velocity and eqs (26) and (32) can be integrated in closed form.

For steady-varied and unsteady flows, eqs (35) and (38) may be solved numerically to yield the free stream flow depth and velocity along the length of the pipe. From this solution local values of F_{ws} and W_b can be obtained and substituted in eqs (26) and (32). Equations (26) and (32) can also be solved numerically. The numerical solutions of these equations are beyond the scope of this study. However, the effects of relevant variables on various states of the solid motion may be examined, without loss of generality, for steady-uniform partially filled pipe flows. The solutions of eqs (26) and (32) and the effects of relevant variables on various states of the motion of a solid are discussed in the following section.

3. Solutions of the Equation of Motion for Steady-Uniform Liquid Flows

The three states of motion of the solid that are considered below include: (1) the threshold conditions, when the motion of the solid is impending; (2) the accelerating motion of the solid, the increase of the velocity of a solid from zero to equilibrium or maximum velocity, U_m , as it travels downstream; and (3) equilibrium velocity conditions, that is, when the solid has attained the equilibrium velocity.

Before proceeding with the solutions of the equation of motion for the solid, it is instructive to describe the relationships of various flow parameters to each other and to the pipe variables for

steady-uniform liquid flows. The volume rate of flow, Q , is considered the controlling flow parameter for this study. For a given value of Q and pipe variables (D , n , and S), the value of flow depth (h) and water velocity (V) can be computed by the use of the Manning equation as [9,10]:

$$Q=(A_w R_w^{2/3} S^{1/2})/n \quad (39)$$

$$V=Q/A_w=(R_w^{2/3} S^{1/2})/n \quad (40)$$

where

$$R_w=(D/4)[1-2(1-2\lambda)(\lambda-\lambda^2)^{1/2}/\cos^{-1}(1-\lambda)] \quad (41)$$

$$\lambda=h/D,$$

and A_w is given in eq (12).

The momentum flux or specific force, M , defined in eq (27), may be computed from h and V . The flow specific energy may also be computed from h and V as:

$$E=h+V^2/2g \quad (42)$$

The quantities h , V , M , and E increase with an increase in Q . For a given flow rate Q , quantity h increases with an increase in n and decreases with an increase in D and S ; the quantities V , M , and E increase with an increase in S and decrease with an increase in D and n . Variations of h and V at a given value of Q , due to variations in D , n , and S would affect various terms in the equation of motion of the solid, i.e., eqs (15), (26), or (32).

3.1 Threshold Conditions

The minimum value of steady-uniform flow rate required to start the motion of a solid, i.e., threshold flow rate, Q_0 , and other threshold flow parameters may be determined by solving eqs (26) and (32) for the threshold conditions, i.e., when the motion of the solid is impending. At threshold conditions, η represents the coefficient of static friction, η_s , between the solid and the pipe wall in the presence of the liquid. The determination of the value of η_s in the presence of the liquid is complex and considered beyond the scope of this study. Nevertheless, η_s is one of the more important variables because it is the major determining factor of the resistance to the motion of a solid. Also, the quantities α , C_r , and U_s are all zero at the threshold conditions. For these conditions, eqs (26) and (32) may be rewritten as:

$$V_o^2-2gL(\sigma A_s/A_{swo}-1)[\eta(1-S^2)^{1/2}-S]/(1+A_{swo}/A_{wo})=0 \quad (43)$$

and

$$V_o^2-\{gL(\sigma A_s/A_{swo}-1)[\eta_s(1-S^2)^{1/2}-S]-g\bar{y}(1-A_{swo}/\sigma A_s)\}=0 \quad (44)$$

where $S=\sin\theta$ =slope of the pipe,

$$A_s=\pi d^2/4,$$

and the other quantities have been previously defined. The free stream liquid velocity V_o , is

related to the free stream water depth h_o , through the free stream hydraulic radius R_o , by the Manning equation as indicated in eq (40).

Substituting for V_o from eq (40), eqs (43) and (44) may be expressed as:

$$(S^{1/2}R^{2/3}/n)^2 - [gL(\sigma A_s/A_{swo}-1)(\eta_s(1-S^2)^{1/2}-S)](A_{swo}/A_{wo}) = 0 \quad (45)$$

and

$$(S^{1/2}R^{2/3}/n)^2 - [gL(\sigma A_s/A_{swo}-1)[\eta_s(1-S^2)^{1/2}-S] - g\bar{y}(1-A_{swo}/\sigma A_s)] = 0 \quad (46)$$

Since the quantities A_{swo} , A_{wo} , R_o , and \bar{y}_o are all functions of the free stream depth, h_o , eqs (45) and (46) may be solved by successive iteration to yield a value of h_o for any values of the variables D , n , S , d , L , σ , and η_s . This value of the stream depth is the threshold stream depth, h_i , and the flow rate corresponding to h_i is the threshold flow rate, Q_i . Knowing the value of h_i , quantity Q_i can be computed by eq (39). The value of threshold flow parameters, i.e., V_i , M_i , and E_i may be computed by the use of appropriate equations.

Equations (45), (46), and (39) are applied to examine the effects of the relevant variables on the threshold flow rate in the following section.

3.1.1 Effects of the Variables on Threshold Flow Rates

Equations (45) and (39) are applied to examine the effects of the variables on Q_i . The seven variables under consideration are D , n , S , d , L , σ , and η_s . The variations of Q_i due to variations in η_s and another variable, while the remaining five variables are held constant are presented in figures 5-11. An examination of these figures indicates that the value of flow rate, Q_i , required to initiate the motion of a solid increase with: an increase in the values of η_s , D , n , d , L , and σ ; and a decrease in the value of S . These results also indicate that for a given solid (i.e., fixed values of d , L , σ , and η_s) and a given value of Q , the chance of initiating the motion of the solid can be increased by selecting a pipe with a smaller diameter and with the lower roughness, (i.e., having a

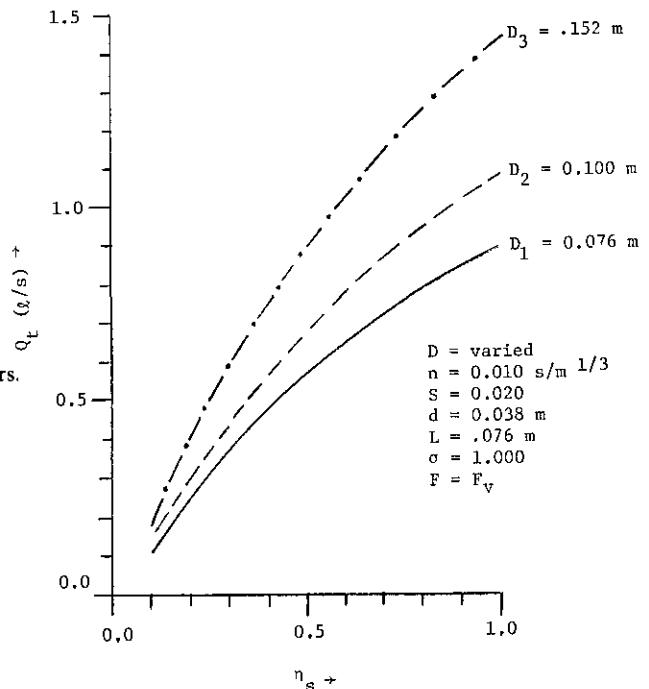


Figure 5- Q_i versus η_s for different values of pipe diameters.

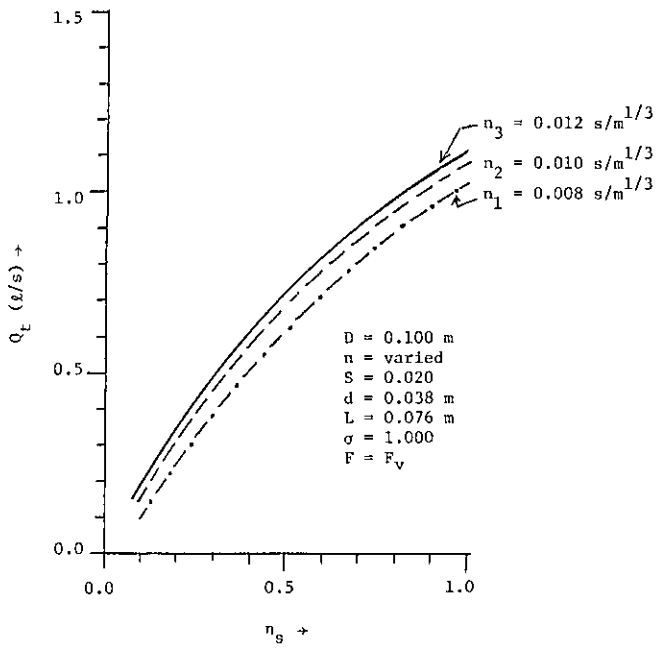


Figure 6— Q_t versus η_s for different values of the Manning coefficient.

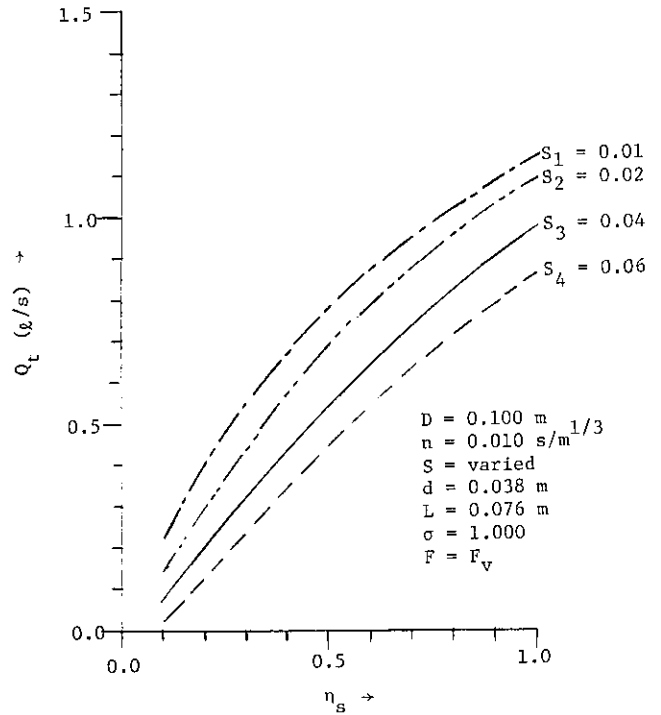


Figure 7— Q_t versus η_s for different values of pipe slope.

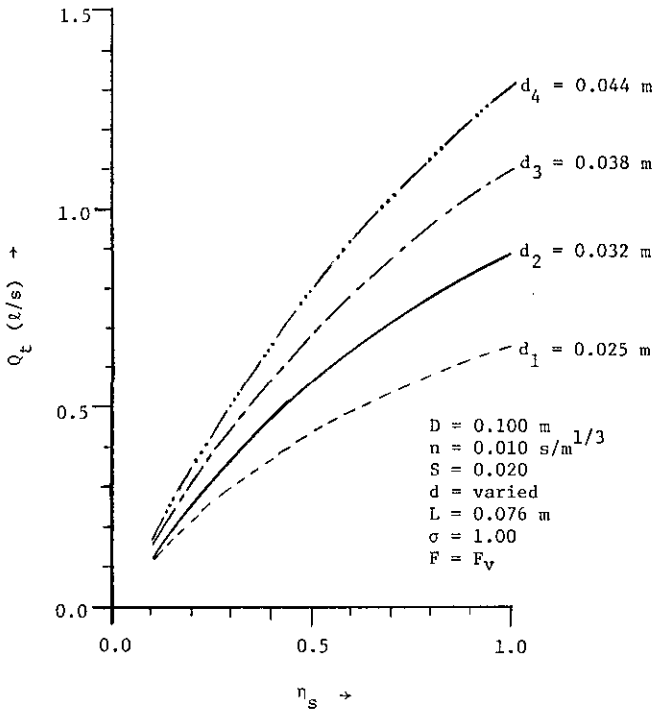


Figure 8— Q_t versus η_s for different values of solid diameter.

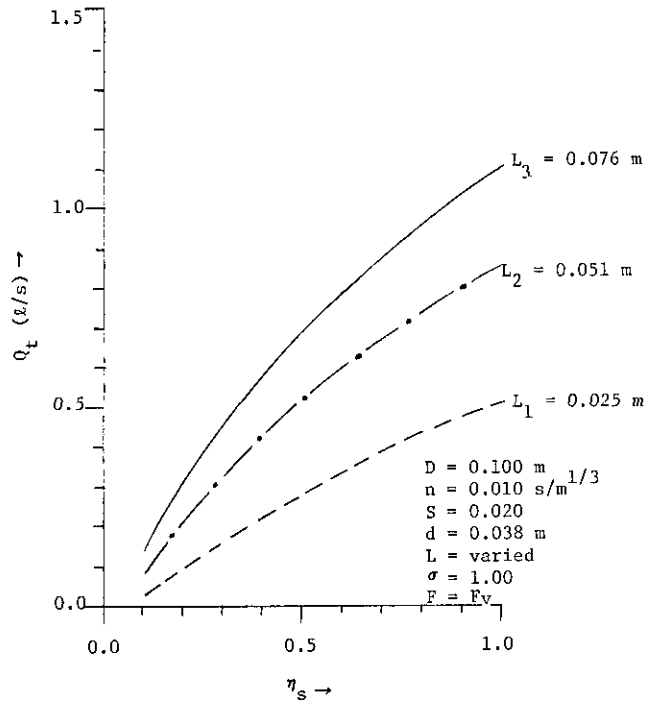


Figure 9— Q_t versus η_s for different values of solid length.

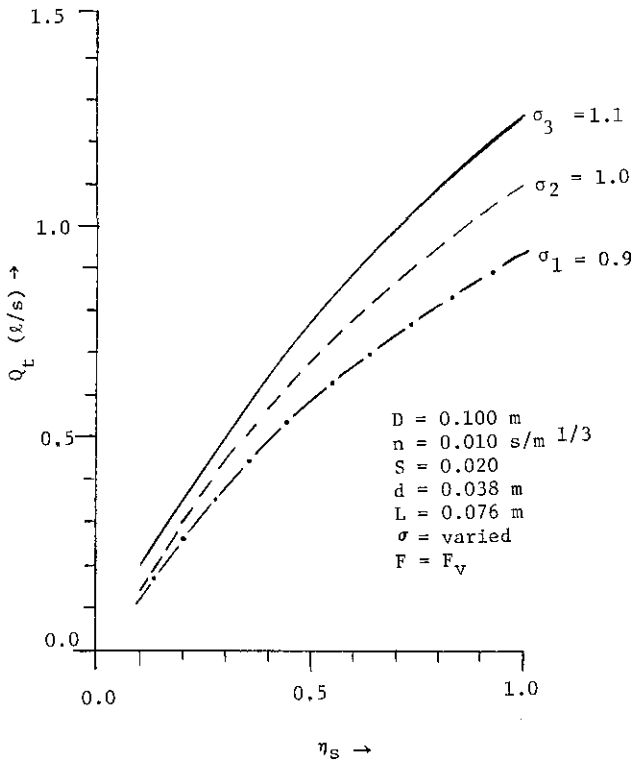


Figure 10— Q_L versus η_s for different values of solid specific gravity.

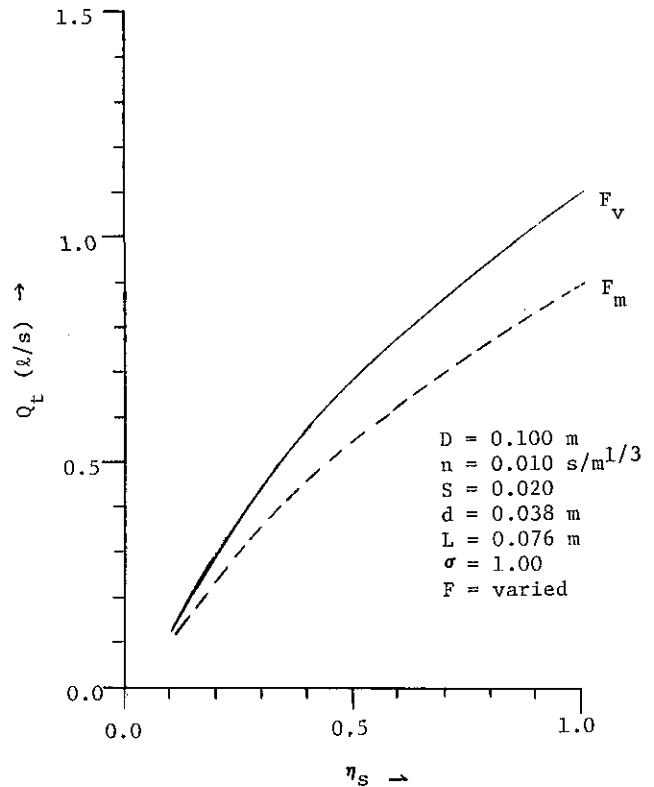


Figure 11— Q_L versus η_s for different force functions.

lower value of the Manning coefficient, n), or by increasing the slope or pitch of the pipe.

Equations (45), (46), and (39) are applied to examine the effects on Q_L of utilizing the two force functions, i.e., the force function F_v based on the free stream velocity (eq (23)) or the force function F_m based on the free stream momentum flux (eq (31)). The variations of Q_L due to variations in η_s , while all other variables are held constant, for the two force functions are shown in figure 11. An examination of this figure indicates that the values of Q_L obtained by the use of F_v are larger than those obtained by the use of F_m . The smaller values of Q_L resulting from the use of force function F_m are consistent with the larger magnitude of force F_{ws} given by F_m than by F_v under identical conditions. It suggests that the selection of a proper force function is an important factor in the development of mathematical models for predicting the motion of solids in partially filled pipes.

3.2 Accelerating Motion of a Solid

Accelerating motion of a solid, i.e., the increase of the velocity of a solid from zero to U_m , as it moves downstream in the pipe may be examined by solving eqs (26) and (32). The lift coefficient, C_L , may be taken as zero without any loss of generality. When the motion of the solid is initiated, η represents the coefficient of kinematic or sliding friction, η_d , between the solid and the pipe wall. Magnitude of η_d is less than that of η_s ; it may vary with the velocity of the solid relative to the pipe wall and it may further decrease if a liquid film is formed between the solid and the pipe wall. However, for the purpose of this study, η_d is considered to be a constant quantity and its value is assumed to be 75% of that of η_s .

Substituting C_1 , equal to zero, $\rho\sigma LA_s$ for the mass of the solid, m , and dU/dT for the acceleration of the solid, α , into eqs (26) and (32) and rearranging the terms the equations may be rewritten as:

$$(V_o - U)^2 - v^2 = 1/N \, dU/dT \quad (47)$$

$$\text{where, } v^2 = 2gL(\sigma A_s / A_{swo} - 1)[0.75\eta_s(1 - S^2)^{1/2} - S] / (1 + A_{swo} / A_{wo}) \quad (48)$$

$$\text{and, } 1/N = 2\sigma LA_s / [A_{swo}(1 + A_{swo} / A_{wo})] \quad (49)$$

and

$$(V_o - U)^2 - v_1^2 = (1/N_1)dU/dT \quad (50)$$

where

$$v_1^2 = gL(\sigma A_s / A_{swo} - 1)[0.75\eta_s(1 - S^2)^{1/2} - S] - g\bar{y}(1 - A_{swo} / \sigma A_s) \quad (51)$$

and

$$1/N_1 = \sigma LA_s / A_{swo} . \quad (52)$$

As indicated earlier, for a given flow rate, the free stream depth and velocity are constant throughout the pipe. Hence, for a given value of Q_o , and the variables D , n , S , d , L , σ , and η_s , the quantities h_o , and V_o are all constants; and the only quantity in eqs (47) and (50) that varies with time is the velocity of the solid, U . Equation (47) may be rewritten as:

$$\frac{dU}{(V_o - U)^2 - v^2} = NdT. \quad (53)$$

The integration of eq (53), for values of v greater than zero and for v equal to zero yields the following:

$$(1/2v)\ln \left(\frac{V_o - U + v}{V_o - U - v} \right) + C_1 = NT, \quad \text{for } v > 0 \quad (54)$$

and

$$1/(V_o - U) + C_2 = NT, \quad \text{for } v = 0 \quad (55)$$

where, C_1 and C_2 are constant, and can be evaluated from the initial condition, i.e., at $T=0$, $U_o=0$. For this initial condition eqs (54) and (55) yield,

$$C_1 = (1/2v) \ln [(V_o + v) / (V_o - v)],$$

and $C_2 = 1/V_o$.

Substituting for C_1 and C_2 in eqs (54) and (55), respectively, and rearranging terms, these equations may be rewritten for U_s as:

$$U = V_o - v \left(\frac{1 + Be^{-bT}}{1 - Be^{-bT}} \right) = \frac{(V_o^2 - v^2) \tanh(bT/2)}{(v + V_o) \tanh(bT/2)}, \quad \text{for } v > 0 \quad (56)$$

and

$$U = V_o^2 NT / (1 + V_o NT), \quad \text{for } \nu = 0 \quad (57)$$

where, $B = (V_o - \nu) / (V_o + \nu)$

and $b = 2 \nu N$.

Equations (56) and (57) give variations of U with time. These equations indicate that the value of maximum velocity attained by a solid is equal to $V_o - \nu$ when ν is greater than zero and V_o when ν is equal to zero.

Equation (56) indicates that U will be equal to U_m at a time, T , for which $\tanh(bT/2)$ is unity or when $bT/2$ is equal to or greater than 6.5. Equation (57) indicates that U will be equal to U_m at a time, T , equal to infinity. Or

$$U_m = V_o - \nu \text{ at } T = 6.5 / \nu N, \quad \text{for } \nu > 0 \quad (58)$$

$$U_m = V_o, \text{ at } T = \infty, \quad \text{for } \nu = 0. \quad (59)$$

Since $U = dX_s / dT$, eqs (56) and (57) may be integrated to determine the distance, X_s , traversed by a solid. Initially, at time T , equal to zero, X_s is zero, for this initial condition integration of eqs (56) and (57) yields the following expressions for X_s ,

$$X_s = (V_o - \nu)T - (1/N) \ln \left(\frac{1 - Be^{-bT}}{1 - B} \right), \quad \text{for } \nu > 0 \quad (60)$$

and

$$X_s = V_o T - (1/N) \ln(1 + V_o NT), \quad \text{for } \nu = 0. \quad (61)$$

Equations (60) and (61) give the variation of X_s with time. Equations (56) and (60) may be applied simultaneously to study the variations of U with the axial distance or as the solid travels downstream from its starting position for ν greater than zero. And for values of ν equal to zero, eqs (57) and (61) may be applied simultaneously to examine the variations of U as the solid travels downstream. Solutions of eq (50), i.e., the expressions for U and X_s corresponding to the force function F_m may be obtained by replacing N and ν by N_1 and ν_1 in eqs (56) to (61). The effects of the variables on the accelerating motion of a solid are examined below.

3.2.1 Effects of the Variables on the Accelerating Motion of a Solid

Equations (56) through (61) are applied to examine the effects of Q and the variables D , n , S , d , L , σ , and η_s on the accelerating motion of the solid. The velocity-histories of a solid, that is, the increase with time of the nondimensional velocity, U/U_m , of a solid from 0.0 to 0.99, are shown in figures 12–20. Each figure shows the effects of one variable on the velocity-history. An examination of these figures indicates the following: (1) the flow rate Q and the variables D , n , S , and σ do not have a significant effect on the velocity-history of a solid; (2) the variables d , L , and η_s do affect the velocity-history, and the time required for U to be equal to U_m increases with an increase in d , L , and η_s ; and (3) the velocity-history is not significantly affected by the force function (fig. 20).

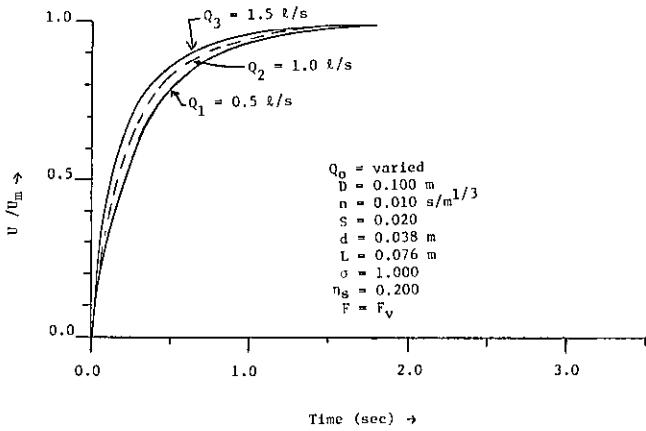


Figure 12—Nondimensional solid velocity, U/U_m , versus time, for different values of flow rate.

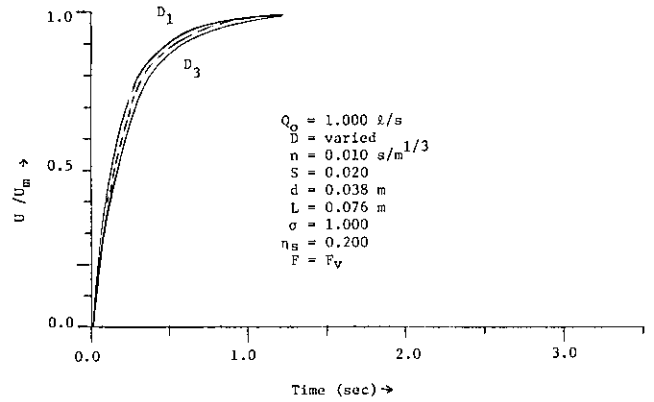


Figure 13—Nondimensional solid velocity, U/U_m , versus time, for different values of pipe diameter.

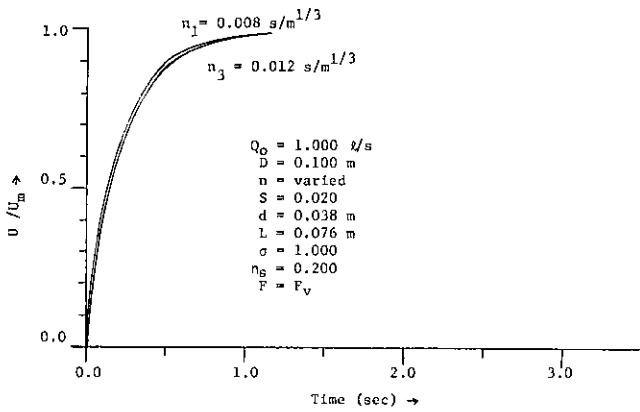


Figure 14—Nondimensional solid velocity, U/U_m , versus time, for different values of Manning coefficient.

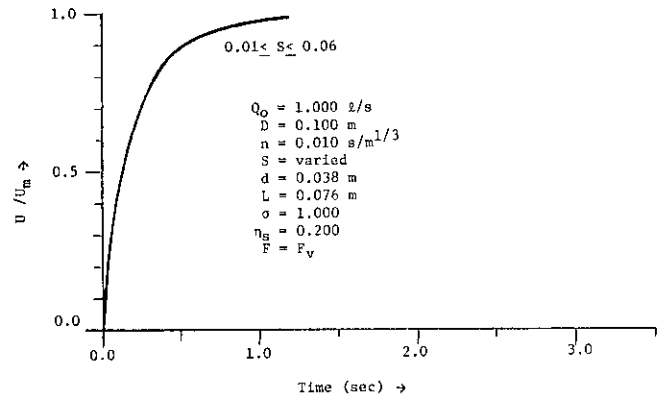


Figure 15—Nondimensional solid velocity, U/U_m , versus time, for different values of pipe slope.

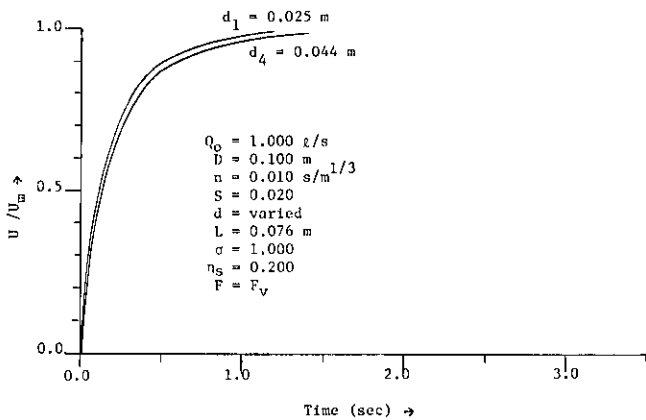


Figure 16—Nondimensional solid velocity, U/U_m , versus time, for different values of solid diameter.

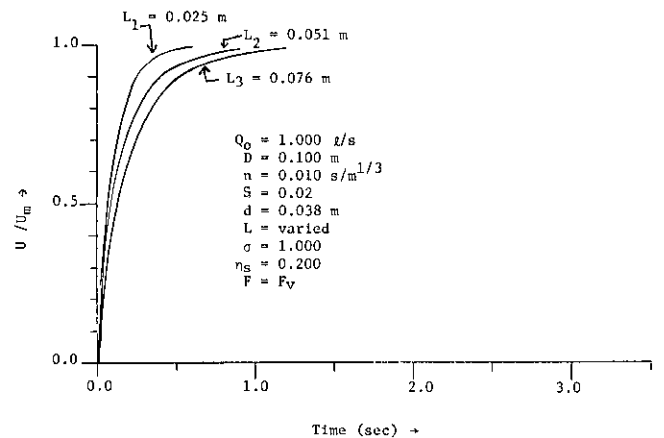
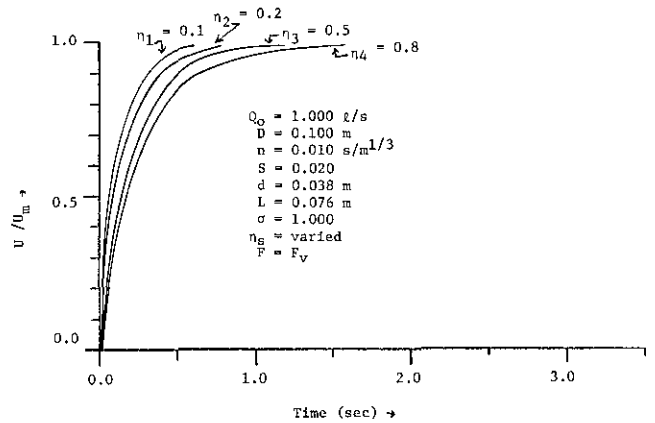
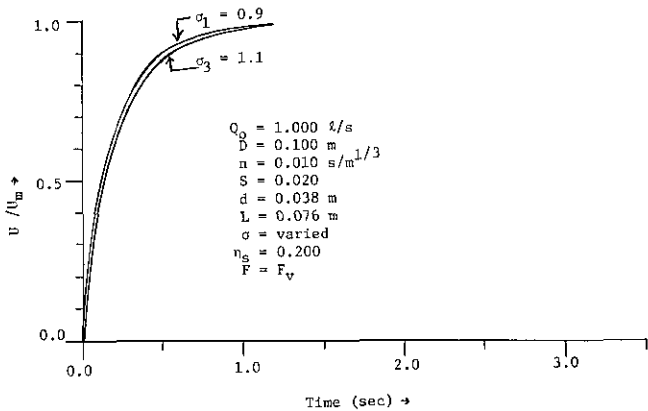


Figure 17—Nondimensional solid velocity, U/U_m , versus time, for different values of solid length.

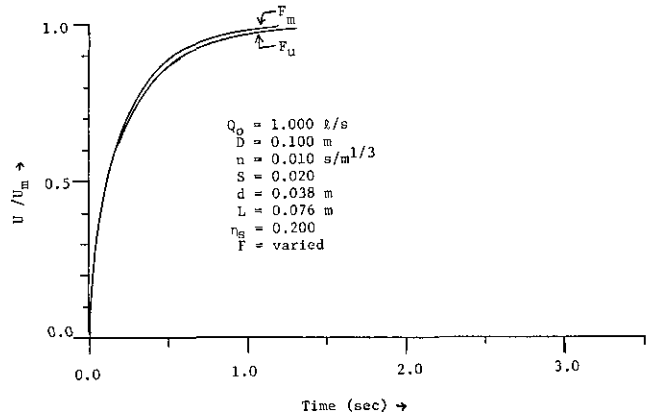


(Clockwise from above)

Figure 18-Nondimensional solid velocity, U/U_m , versus time, for different values of solid specific gravity.

Figure 19-Nondimensional solid velocity, U/U_m , versus time, for different values of η_s .

Figure 20-Nondimensional solid velocity, U/U_m , versus time, for different force functions.

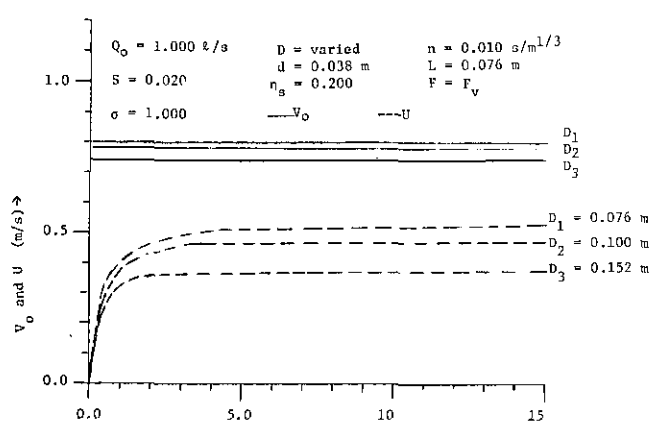
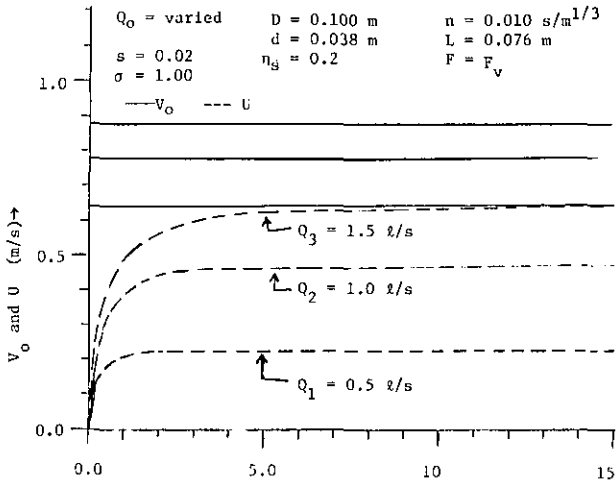


The velocity-distance profiles of a solid, that is, the variation of the velocity of a solid with the nondimensional axial distance, X/D , traversed by the solid are shown in figures 21-29. Each of these figures shows the effect of one of the variables (Q , D , n , S , d , L , σ , η_s , and F_v or F_m) on the velocity-distance profile of a solid. An examination of these figures indicates the following: (1) the distance traversed by a solid during its acceleration from rest to a velocity of $0.99 U_m$ increases with an increase in Q , S , and L , and decreases with an increase in D , n , d , σ , and η_s ; (2) the velocity, U , of a solid at a given axial distance increases with an increase in Q and S ; (3) the value of U at a given axial distance decreases with an increase in D , n , d , L , σ , and η_s ; and (4) the velocities of a solid at all axial distances are higher when F_m is used than when F_v is used.

3.3 Equilibrium Velocity Conditions

The equilibrium velocity of a solid, for steady-uniform flow is a constant quantity, and it is the maximum velocity that a solid can attain for a given value of flow rate. The expression for the equilibrium or maximum velocity, U_m , is given in eq (58) for $\nu > 0$, and in eq (59) for $\nu = 0$. The expression for U_m may also be obtained by letting dU/dT equal to zero in eqs (47) and (50), and are:

$$U_m = V_o - \nu, \text{ for force function } F_v, \quad (63)$$



(Clockwise from above)

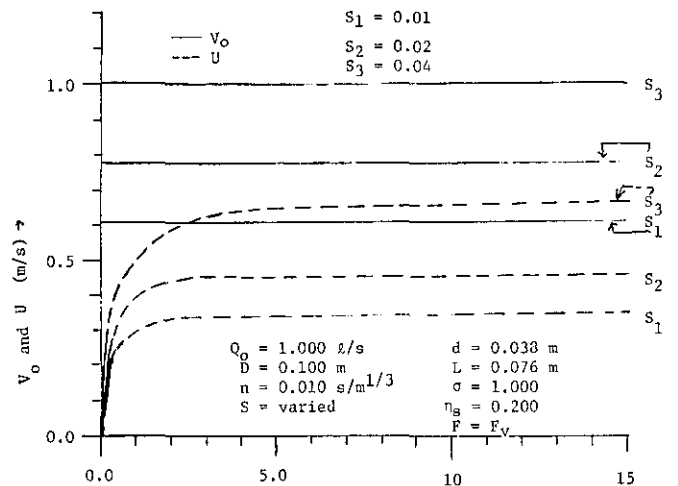
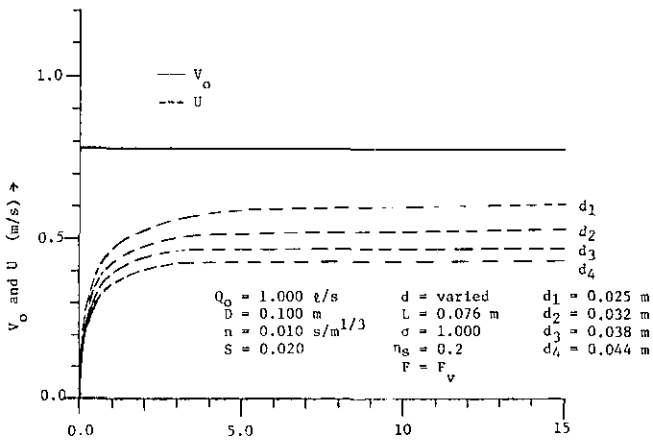
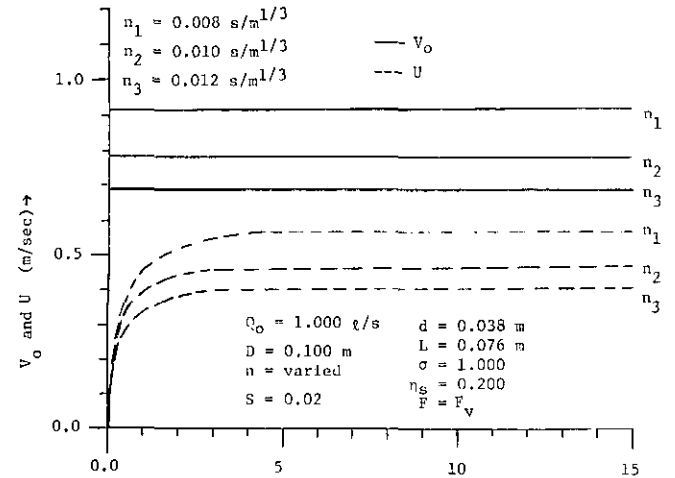
Figure 21—Solid velocity versus nondimensional axial distance, for different values of flow rate.

Figure 22—Solid velocity versus nondimensional axial distance, for different values of pipe diameter.

Figure 23—Solid velocity versus nondimensional axial distance, for different values of Manning coefficient.

Figure 24—Solid velocity versus nondimensional axial distance, for different values of pipe slope.

Figure 25—Solid velocity versus nondimensional axial distance, for different values of solid diameter.



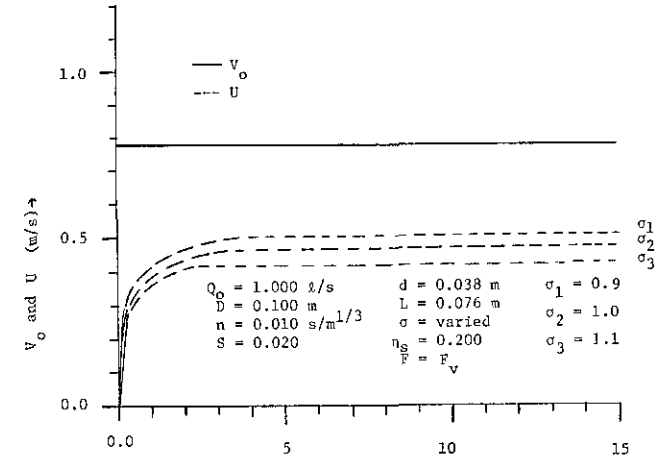
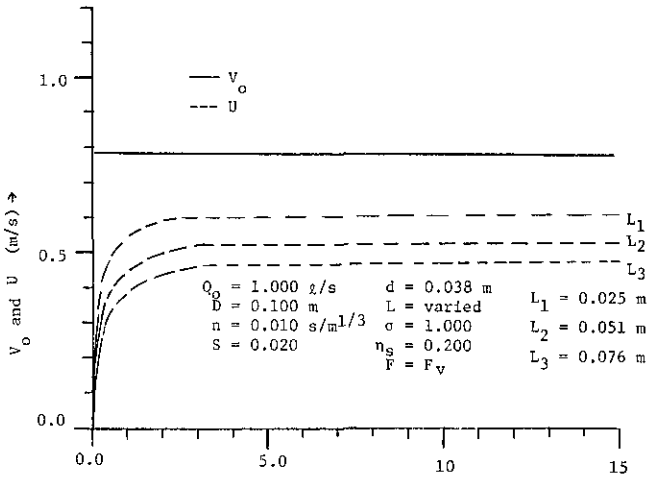


Figure 26—Solid velocity versus nondimensional axial distance, for different values of solid length.

Figure 27—Solid velocity versus nondimensional axial distance, for different values of solid specific gravity.

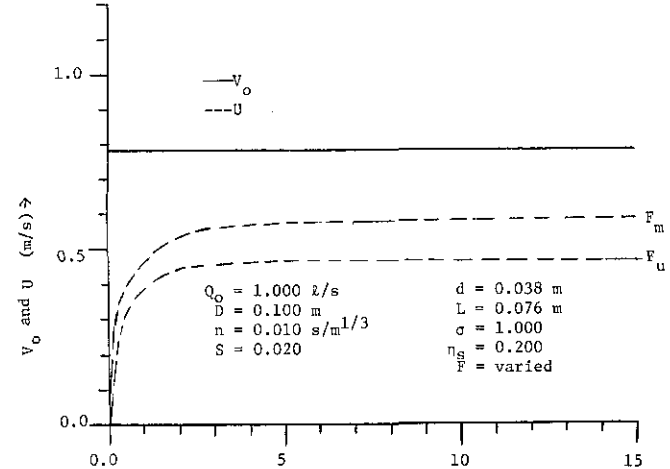
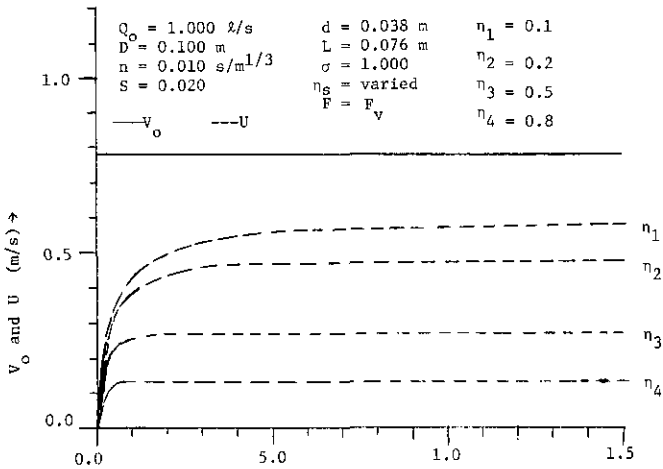


Figure 28—Solid velocity versus nondimensional axial distance, for different values of η_c .

Figure 29—Solid velocity versus nondimensional axial distance, for different force functions.

and

$$U_m = V_o - v_1, \text{ for force function } F_m, \quad (64)$$

where, v and v_1 are given in eqs (49) and (52), respectively.

The effects of the variations of flow rate Q and various variables U_m are examined below.

3.3.1 Effects of the Variables on the Maximum Velocity of a Solid

Equations (39), (44), and (63) are applied to examine the effects of the liquid flow rate, Q , and of the variables D , n , S , d , L , σ , and η_s on U_m . The variations of U_m due to variations of Q and one variable, while the other six variables are held constant, are shown in figures 30–37. The

corresponding variations of V_o are also shown in these figures for comparison. The maximum value of Q considered for this study is equal to 2.0 l/s (or about 31.4 gal/min); this value of Q corresponds to the approximate value of the peak water flow rate from water closets. An examination of these figures indicates the following: (1) both V_o and U_m increase with an increase in Q ; (2) as indicated earlier, flow velocity, V_o , increases with an increase in S and a decrease in D and n ; and (3) the maximum velocity of solid, U_m , increases with an increase in S , and it decreases with an increase in D , n , d , L , σ , and η_s .

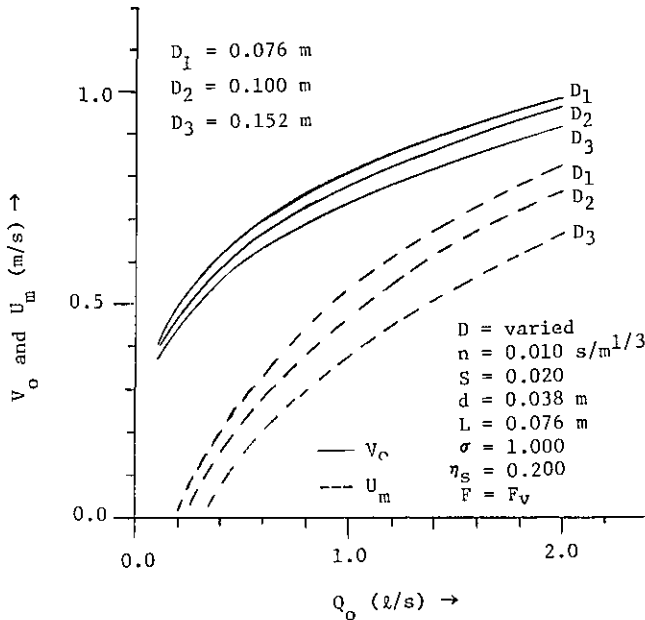


Figure 30-The maximum velocity, U_m , of a solid versus Q_o , for different values of pipe diameter.

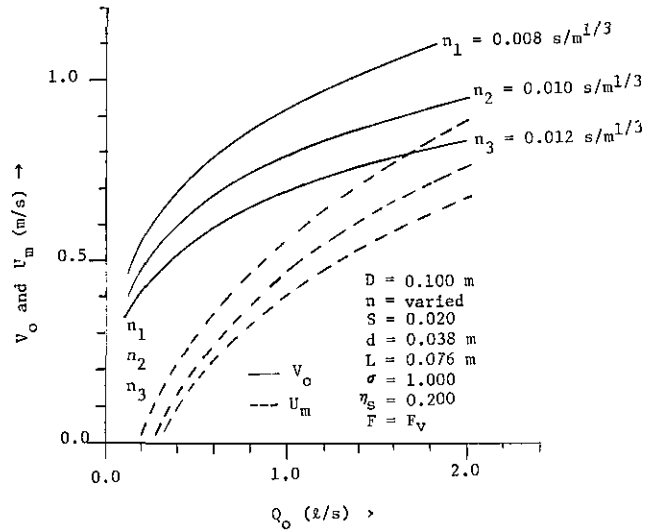


Figure 31. The maximum velocity, U_m , of a solid versus Q_o for different values of pipe diameter

Figure 31-The maximum velocity, U_m , of a solid versus Q_o , for different values of Manning coefficient.

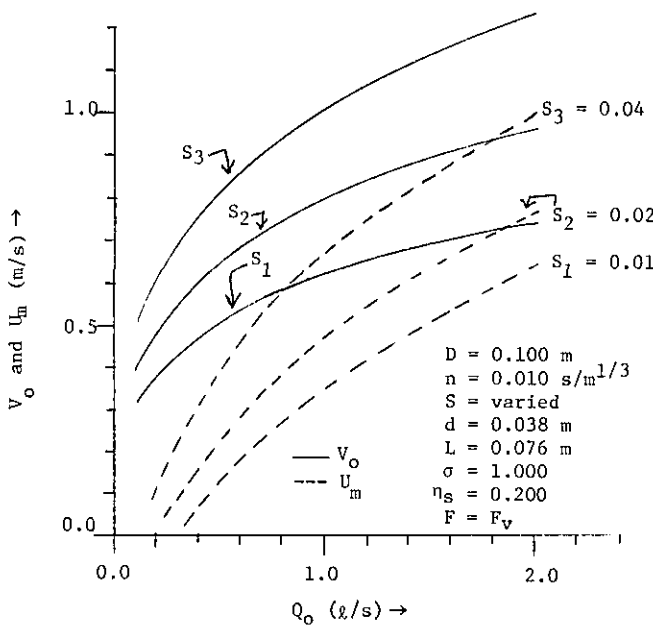


Figure 32-The maximum velocity, U_m , of a solid versus Q_o , for different values of pipe slope.

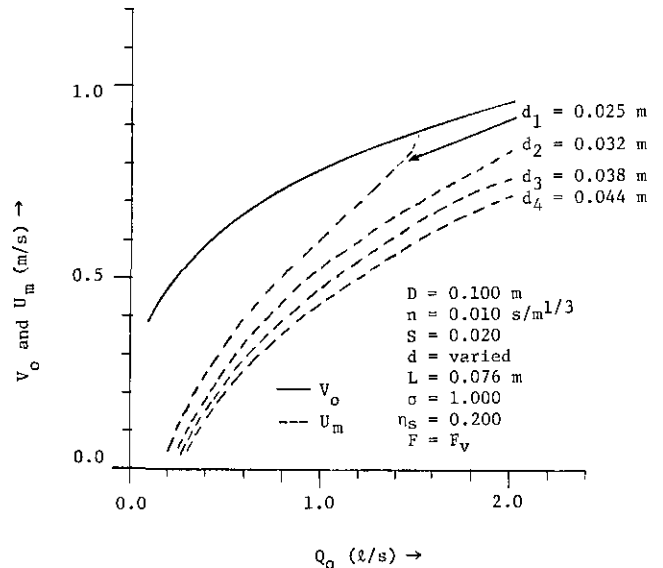


Figure 33-The maximum velocity, U_m , of a solid versus Q_o , for different values of solid diameter.

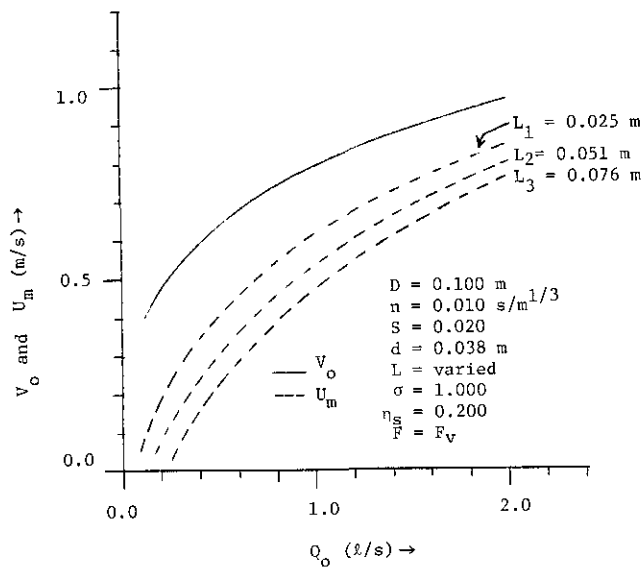


Figure 34—The maximum velocity, U_m , of a solid versus Q_o , for different values of solid length.

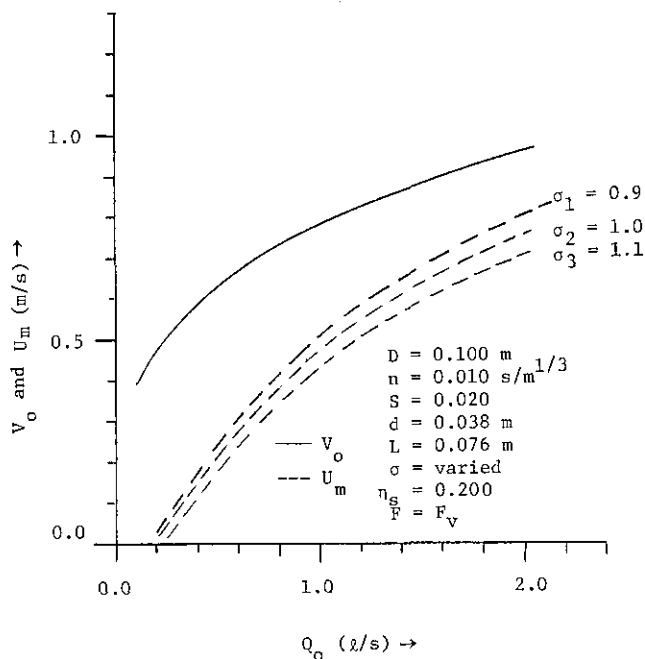


Figure 35—The maximum velocity, U_m , of a solid versus Q_o , for different values of solid specific gravity.

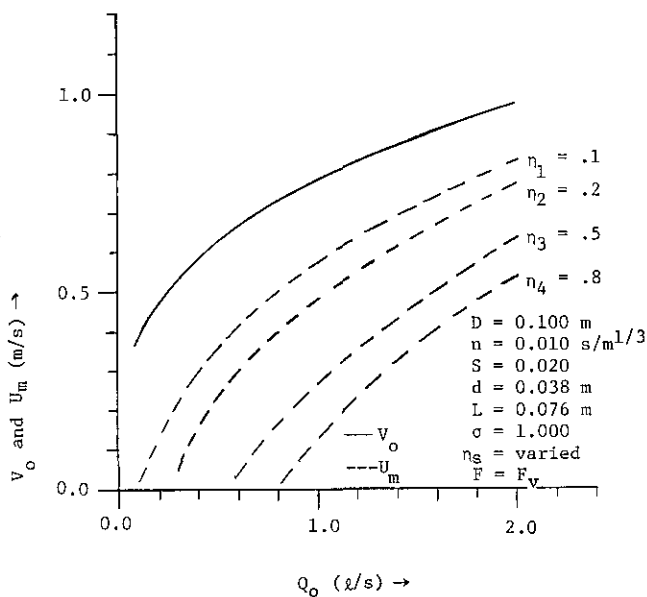


Figure 36—The maximum velocity, U_m , of a solid versus Q_o , for different values of η_s .

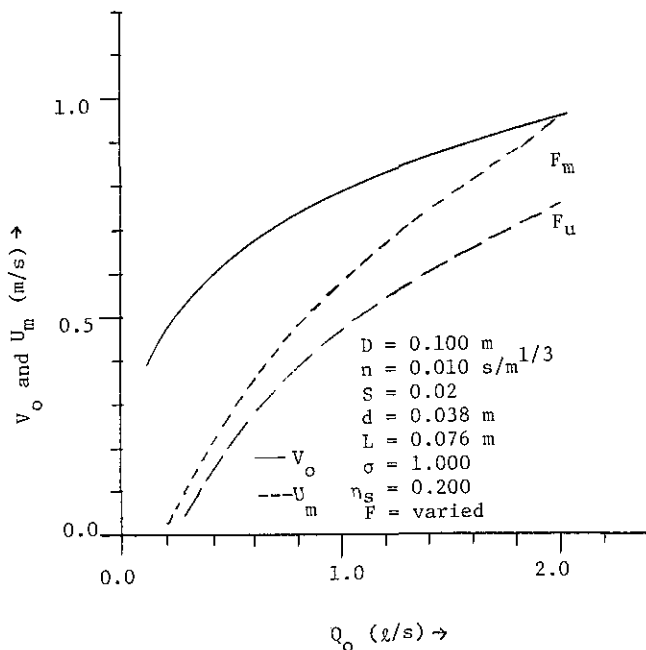


Figure 37—The maximum velocity, U_m , of a solid versus Q_o , for different force functions.

Equations (63) and (64) are applied to examine the effects of the two force functions on U_m . The variations of U_m due to variations of Q , for a set of values of the variables are shown in figure 37. An examination of this figure indicates the values of U_m are higher for F_m than those for F_v . The larger values of U_m attained by a solid when force function F_m is used, are consistent with the larger magnitude of force given by F_m than by F_v under identical conditions.

3.4 Comparison with Experimental Data

An experimental study of the motion of single solids with steady uniform flows in partially filled pipes was carried out under the sponsorship of NBS at Brunel University, U.K. [16]. In this study, the solid was introduced into the established flow with some initial velocity via a 50 mm tube and a 45° elbow and the effects of some variables (Q , S , L , d , and σ) on the velocity of the solid (U) were examined. The details of the experimental equipment and procedures may be found in reference [16]. Examples of typical data from reference [16] are reproduced in figures 38 and 39.

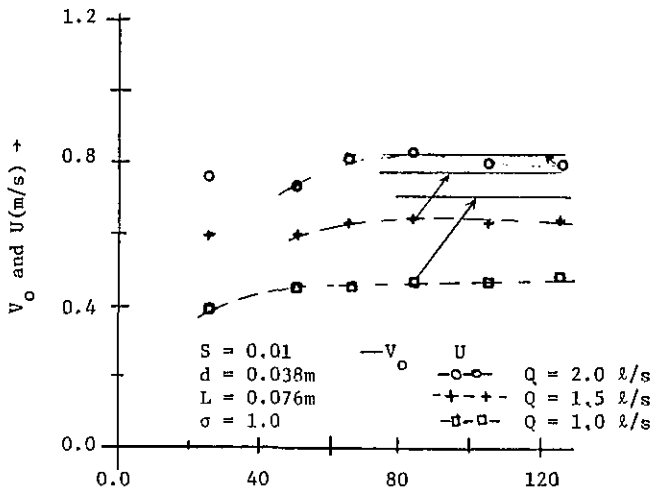


Figure 38—Solid velocity measured along the 100 mm diameter pipe compared with the free stream water velocity (Ref. 16).

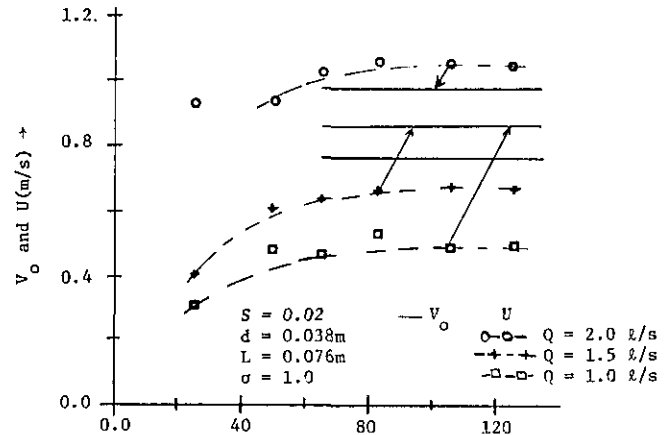


Figure 39—Solid velocity measured along the 100 mm diameter pipe compared with the free stream water velocity (Ref. 16).

The experimental data indicate that the effects of the variables (Q , S , L , d , and σ) on the solid velocity predicted by the analysis (figs. 21–29) are qualitatively consistent with the data of reference [16]. The observed values of the maximum solid velocity are fairly close to the results predicted by eqs (56) through (59) for the magnitude of η_s equal to about 0.1, except for the experiments with a flow rate of 2 l/s. The data for the flow rates of 2 l/s indicate that the solid velocity (U) is somewhat higher than the free stream velocity (V_o) of the carrier liquid calculated from the measured values of flow depth. These results may be explained as follows.

When the quantity $W_b(1-C_f)$ is equal to zero, then the solid no longer drags on the pipe wall but moves as a waterborne object situated in the flow somewhere above and away from the pipe wall. The free stream velocity (V_o), calculated by the Manning equation or by the measured flow depth, represents the average value of the flow velocity averaged over the wetted portion of the cross-section area. Considering the velocity distribution of a partially filled pipe flow at a pipe cross-section, the value of average velocity, V_o may be somewhat less than the velocity of the liquid adjacent to the waterborne solid moving with velocity, U . However, the available data are too few to draw any definite conclusions.

Equations (56) through (59) are not capable of predicting this phenomenon. Since the analysis leading to these equations has been based on free stream conditions derived from the Manning equation, it limits the maximum value of U to V_o .

Typical data showing the velocity of single solids induced by surge flows in a partially filled pipe are reproduced from reference [4] in figures 40 and 41. The effects of the variables (D , S , L ,

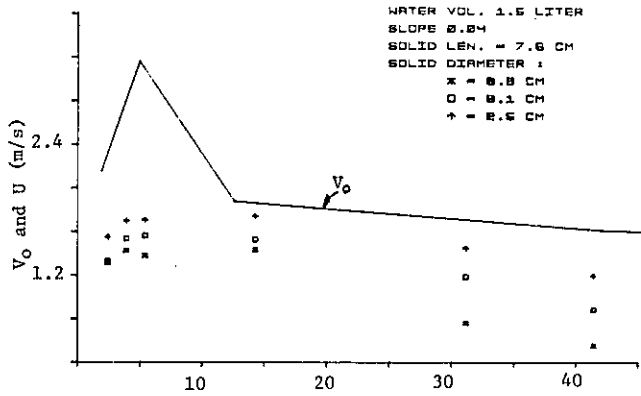


Figure 40—Solid velocity versus nondimensional axial distance for 7.6 cm long solids and for water volume=1.5 L, and $S=0.04$ (Ref. 4).

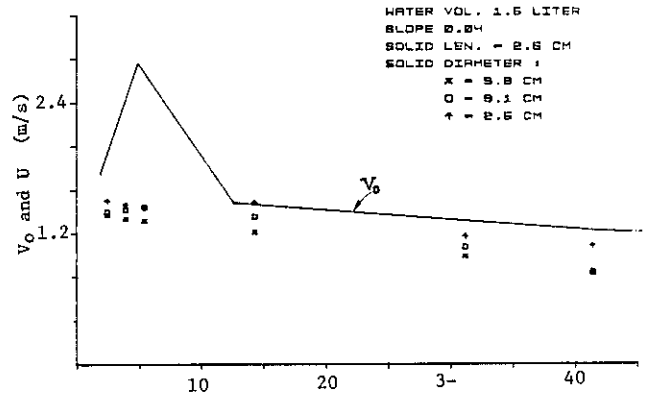


Figure 41—Solid velocity versus nondimensional axial distance for 2.5 cm long solids and for water volume=1.5 L, and $S=0.04$ (Ref. 4).

d , and η_s), predicted by the analysis for steady uniform flow are also qualitatively consistent with the data of references [3] and [4].

The qualitative consistency between the predicted and observed effects of variables on the flow-induced velocity of a solid confirms the form of the analysis presented. The available experimental data also illustrate the limitations of the model inherent in the use of free stream velocity derived from a one-dimensional representation of flow such as the Manning equation.

4. Conclusions

A general equation for the liquid flow-induced motion of a solid is developed. Two alternate force models, one based on free stream velocity and the other on free stream momentum flux, are formulated to approximate the flow-induced force acting on the solid. These force models simplify the equation of motion. The simplified equation is solved for steady uniform liquid flows to examine the effects of flow rate (Q), pipe variables (D , n , and S), solid variables (d , L , and σ), coefficient of friction between solid and pipe wall (η_s), and the force functions (F_v or F_m) on the motion of the solid.

The minimum value of flow rate required to initiate the motion of a solid, or the threshold flow rate, increases with an increase in D , n , d , L , σ , and η_s and decreases with an increase in S . The flow rates required to initiate the motion of solid predicted by the use of F_v are larger than those predicted by the use of F_m .

The maximum velocity attained by a solid as well as the velocity of the solid at a given axial distance of the pipe increase with an increase in Q_0 and S , and decrease with an increase in D , n , d , L , σ , and η_s . The qualitative effects of the variables Q_0 , D , S , d , L , and η_s on the velocities of the solids are consistent with the available experimental data. The velocities of a solid predicted by the use of F_v are lower than those predicted by F_m .

The qualitative consistency between the predicted and observed effects of the different variables on the motion of the solid demonstrates the validity of the analysis presented. To obtain quantitative agreement between the predicted and experimental results, and to determine which of the two force models is better suited for the problem it is necessary to determine or assume the values of the coefficient of friction between a solid and the pipe wall in the presence of the liquid.

References

- [1] Yalin, M. S. *Mechanics of sediment transport*. New York: Pergamon Press; 1972.
- [2] Govior, A. W.; Azia, K. *The flow of complex mixtures in pipes*. New York: Van Nostrand Reinhold Company; 1972.
- [3] Mahajan, Bal M. Experimental investigation of transport of finite solids in a 76 mm-diameter partially-filled pipe. Natl. Bur. Stand. (U.S.) NBSIR 81-2266; 1981 April.
- [4] Mahajan, Bal M. Experimental investigation of transport of discrete solids with surge flows in a 10.0 cm diameter partially-filled pipe. Natl. Bur. Stand. (U.S.) NBSIR 81-2450; 1982 January.
- [5] Karnata, M., et al. Studies on flow and transport of feces in horizontal waste pipes. Proc. of the CIB W62 Seminar on Drainage and Water Supply in Buildings, Paris, France; 1979 November.
- [6] Swaffield, J. A.; Marriott, B. S. T. An investigation of the effects of reduced volume W. C. flush on the transport of solids in above ground drainage systems. Proc. of CIB W62 Symposium, Brussels, Belgium; 1978 May.
- [7] Swaffield, J. A.; Wakelin, R. H. M. A study of the interaction of drainage system loading and reduced flush W. C. operation. Proc. of the CIB W62 Seminar on Drainage and Water Supply in Buildings, Paris, France; 1979 November.
- [8] Swaffield, J. A. Application of the method of characteristics to model the transport of discrete solids in partially filled pipe flow. Natl. Bur. Stand. (U.S.) Bldg. Sci. Ser. 139; 1982 February.
- [9] Chow, V. T. *Open-channel hydraulics*. New York: McGraw-Hill Book Company; 1959.
- [10] Henderson, F. M. *Open channel flow*. New York: The MacMillan Company; 1967.
- [11] Ackers, P.; Harrison, J. M. Attenuation of flood waves in part-full pipes. Proc. I.C.E. (London), Vol. 28; 1964 July.
- [12] Price, R. K. Comparison of four numerical methods for flood routing. HY7—July 74: 879: 10659.
- [13] Swaffield, J. A. An initial study of the application of the numerical method of characteristics to unsteady flow analysis in partially filled gravity drainage sized pipes. Natl. Bur. Stand. (U.S.) NBSIR 81-2308; 1981 July.
- [14] Rouse, H. *Elementary mechanics of fluids*. New York: John Wiley and Sons, Inc.; 1964.
- [15] John, J. E. A.; Haberman, W. *Introduction to fluid mechanics*. Englewood, N.J.: Prentice-Hall, Inc.; 1971.
- [16] Swaffield, J. A.; Bridge, S.; Galowin, L. S. Mathematical modeling of time dependent wave attenuation and discrete solid body transport in gravity driven partially filled pipe flows. Brunel University Report No. DREG/NBS/6, 1982 January.